Investigation of Intermodal Four-Wave Mixing for Continuous-Wave Photon-Pair Generation

Seyedehnajmeh Montazeri, Md. Abu Zobair, and Mina Esmaeelpour, Member, IEEE

Abstract—We experimentally demonstrate the various intermodal and intramodal four-wave mixing processes in a few-mode fiber with three modes using non-degenerate pumps. We distinguish the processes by calculating their phase mismatch and identify the intermodal spontaneous four-wave mixing process that generates entangled photon pairs in various modes. We achieve this using continuous-wave beams and the seeding technique due to the low efficiency of the spontaneous four-wave mixing effect in the fiber. We seeded the Stokes and anti-Stokes waves and measured the spectral content of each mode while moving the seed away from the perfect phase-matched condition in the fiber under test. We observe that the closer the seed gets to the pumps, the higher the efficiency of the four-wave mixing process.

Index Terms—Spontaneous four-wave mixing, few-mode fiber, nonlinear fiber optics, quantum entangled laser source.

I. Introduction

OR the first time, the intermodal four-wave mixing (FWM) was observed by Stolen et al. [1], where they used the different group velocity dispersions of various spatial modes to achieve phase matching in a multimode fiber (MMF). Since then, the prospect of using the spatial mode contents of optical fibers to increase the transmission bandwidth in optical communication systems triggered interest in understanding nonlinear effects in MMFs and few-mode fibers (FMFs), resulting in renewed interest in the topic [2]. Until recently, many studies of intermodal fiber nonlinearities have focused on highly nonlinear and photonic crystal fibers with short lengths [3], [4]. Xiao et al. theoretically studied this effect in a telecommunication length FMF, taking into account the random mode-coupling and studying the bandwidth and the phase-matching condition [5]. Esmaeelpour et al. fully characterized the stimulated intermodal FWM in the same fiber, measuring the effects' bandwidth, polarization dependence, and power fluctuations [6]. Since then, many studies have focused on stimulated and spontaneous FWM (SFWM) in MMFs and FMFs [7], [8].

While the FWM effect is to be avoided in communication applications, it is desired in applications such as wavelength conversion and parametric amplification [9], [10]. Additionally, intermodal SFWM can be presented as the source of

Manuscript received 4 March 2024; accepted 18 March 2024. Date of publication 4 April 2024; date of current version 9 April 2024. This work was supported in part by the National Science Foundation (NSF) under Grant 2301870. (Corresponding author: Mina Esmaeelpour.)

The authors are with the Electrical and Computer Engineering Department, Missouri University of Science and Technology, Rolla, MO 65409 USA (e-mail: me96d@mst.edu).

Color versions of one or more figures in this letter are available at https://doi.org/10.1109/LPT.2024.3382688.

Digital Object Identifier 10.1109/LPT.2024.3382688

entangled photon pairs. The most common technique for generating quantum-mechanically entangled photons is spontaneous parametric down-conversion using second-order nonlinearities in bulk crystals [11]. Photon pair generation has also been demonstrated using third-order nonlinearities in single-mode fibers using high-power pulsed lasers [12]. Recently, the SFWM process in graded index FMFs and MMFs as a source of entangled photon pairs has become a topic of interest [13], [14], [15], [16], [17], [18]. Many of these studies have mainly focused on using pulsed laser sources due to the low efficiency of intermodal FWM effect as well as better manage spontaneous Brillouin scattering (SBS) of the fiber with spectrally broad laser sources.

Here, we investigate intermodal SFWM in a 25 km FMF with three spatial modes using tunable non-degenerate continuous wave (CW) pumps having the flexibility to study various spatial modes and wavelength configurations to characterize the effect and understand optimal FWM conditions for photon pair generation. The present letter reports our progress over [19] providing our results and technique to identify the source of the FWM effect at the presence of strong coupling between modes using the seeding technique in the search for optimal phase matching condition for photon-pair generation through intermodal SFWM.

II. SPONTANEOUS FOUR-WAVE MIXING THEORY

In this section, we study phase-matching conditions for the non-degenerate SFWM in an FMF. In this work, we used an FMF that supports three spatial linearly polarized (LP) modes known as LP₀₁, LP_{11a}, and LP_{11b}, resulting in six polarization modes in total. Assuming that the two pumps coupled in the fiber within two different modes of LP₀₁ and LP₁₁ through SFWM, we expect two extra frequencies to be generated, identified as ω_s and ω_{as} for the Stokes and anti-Stokes frequencies in the LP₁₁ and LP₀₁ modes, respectively. The phase matching condition must be met for the SFWM to take place. The energy conservation equation, $\omega_s^{01} + \omega_{as}^{11} = \omega_{p1}^{01} + \omega_{p2}^{11}$, and the momentum conservation equation, $\beta_s^{01} + \beta_{as}^{11} = \beta_{p1}^{01} + \beta_{p2}^{11}$, can be used to determine the optical angular frequencies of the Stokes and anti-Stokes signals that will be generated through the SFWM process. Here, β is the propagation constant, and ω is the angular frequency. The pumps, Stokes, and anti-Stokes signals are identified by the designations p1, p2, s, and as subscripts, respectively. The corresponding mode of each frequency component is shown as a superscript, with 01 corresponding to LP₀₁ mode and 11 for the LP₁₁ mode group. To find the Stokes and anti-Stokes

1041-1135 © 2024 IEEE. Personal use is permitted, but republication/redistribution requires IEEE permission. See https://www.ieee.org/publications/rights/index.html for more information.

frequencies, we apply the Taylor expansion to $\beta\left(\omega\right)$ around an arbitrary frequency ω_{0} , as $\sum_{n=0}^{\infty}\beta_{n}\mid_{\omega=\omega_{0}}\left(\omega-\omega_{0}\right)^{n}/n!$, where $\beta_{n}=\left(d^{n}\beta/d\omega^{n}\right)\mid_{\omega=\omega_{0}}$ is the nth-order dispersion in the Taylor series expansion of the propagation constant, β , around an arbitrary frequency, ω_{0} . We truncate the series at the third-order term of the Taylor expansion. $\beta_{1}=1/v_{g}$ is the inverse group velocity, and $\beta_{2}=d\beta_{1}/d\omega$ at $\omega=\omega_{0}$. The optimal phase matching condition for the SFWM process can then be calculated as in (1). Together with the energy conservation equation $\omega_{s}^{01}+\omega_{as}^{11}=\omega_{p1}^{01}+\omega_{p2}^{11}$ equation, and defining $\Delta\omega=\omega_{k}-\omega_{0}$ for $k\in\{s,as,p1,p2\}$, we can find the expected Stokes and anti-Stokes frequencies for specific pump frequencies by solving the below equation.

$$\beta_1^{11} + \frac{\beta_2^{11}}{2} \left(\Delta \omega_{as} + \Delta \omega_{p2} \right) = \beta_1^{01} + \frac{\beta_2^{01}}{2} (\Delta \omega_{p1} + \Delta \omega_s)$$
(1)

This effect was previously identified with the nomenclature "PROC 2" in [19] for stimulated intermodal FWM in an FMF. Knowing the fiber's group velocity, group velocity dispersion, and the applied pumps' frequencies, we can find the expected frequencies for the Stokes and anti-Stokes processes through the SFWM at the optimal phase matching condition. Since we have previously demonstrated that the intermodal FWM has a large bandwidth of at least a few nanometers [5], we can still observe the FWM but at a lower efficiency, even if we are not at the optimal condition. To identify the degree of phase-matching of an effect that is experimentally observed, we define phase-mismatch for SFWM written as $\Delta\beta = \beta_s^{01} + \beta_{as}^{11} - \beta_{p1}^{01} - \beta_{p2}^{11}$. For the specific process of intermodal SFWM in an FMF, the phase-mismatch can be written as (2) by expanding β (ω) and truncating to the third-order term of the Taylor series for simplicity as

$$\Delta\beta \approx \beta_1^{11} \left(\Delta\omega_{as} - \Delta\omega_{p2} \right) + \frac{\beta_2^{11}}{2} \left(\Delta\omega_{as}^2 - \Delta\omega_{p2}^2 \right) - \beta_1^{01} (\Delta\omega_{p1} - \Delta\omega_s) - \frac{\beta_2^{01}}{2} (\Delta\omega_{p1}^2 - \Delta\omega_s^2). \quad (2)$$

The Stokes and anti-Stokes frequencies resulting from the intermodal SFWM process are shown to have very low efficiency. Therefore, to confirm the phase-matching processes, we calculate the expected frequencies of these effects and their corresponding modes based on the intermodal phase-matching process of (1) and seed one of the processes to observe the second one.

III. SPONTANEOUS FOUR-WAVE MIXING EXPERIMENT

The FMF that was used for the experimental studies was a 25-km long, graded index FMF from OFS Optics Inc. The fiber has an average loss coefficients of 0.23 dB/km, and its group velocity has been previously reported in [20] with an average differential group delay of $\sim 60 \text{ps/km}$ resulting in a $\Delta\lambda = \lambda^{11} - \lambda^{01} = 3.2$ nm between the two modes to have equal inverse group velocities within the C band. $\Delta\lambda$ is the relative wavelengths of signals in the LP₀₁ and LP₁₁ modes to have the same group velocity. λ^{11} is the wavelength in LP₁₁ mode and λ^{01} is the wavelength in LP₀₁ mode. In this

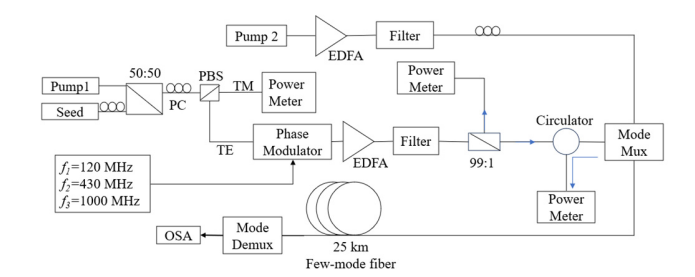


Fig. 1. Experimental Setup for intermodal SFWM studies in FMFs; PC: polarization controller, PBS: Polarization beam splitter, EDFA: erbium-doped fiber amplifier, and OSA: optical spectrum analyzer.

fiber, LP_{11a} and LP_{11b} modes are degenerate. In search of the intermodal SFWM process, we carefully chose the pumps' frequencies using (1). Figure 1 illustrates the experimental configuration for investigating the intermodal SFWM in the fiber under test. The setup employs two CW external cavity lasers as high-power pumps, p1 and p2, injected into the LP₁₁ and LP₀₁ modes by coupling them into LP_{11a} and LP₀₁ ports of the all-fiber mode multiplexer, respectively. Two allfiber spatial mode multiplexers known as "photonic lanterns" are utilized to guide the waves into and out of a designated spatial mode of the FMF with 1 dB insertion loss in the LP₀₁ and 1.7 dB in the LP_{11a/b} inputs. Crosstalk of 14.36 dB from LP₀₁ to LP₁₁ ports and 15.86 dB from LP₁₁ ports to LP₀₁ port are measured. Choosing $\lambda_0 = 1555$ nm, from which we can find $\omega_0 = 2\pi c/\lambda_0$, the relative β_1 at $\omega = \omega_0$ is found to be $\beta_1^{11} - \beta_1^{01} = -60.94$ ps/km. Also, β_2 values for both modes are found to be $\beta_2^{01} = -24.3774$ ps²/km and $\beta_2^{11} = -24.2832 \text{ps}^2/\text{km} \text{ at } \omega = \omega_0$ [20].

Pump 1 and seed signal are combined through a polarization beam splitter (PBS). Polarization controllers after each laser and after the transverse electric (TE) output of the PBS are used to maximize the combined power and parallelize the polarization of two beams before they enter a phase modulator. Phase dithering with 120, 430 and 1000 MHz tones are applied to increase the SBS threshold of the FMF by 8 dB. It is worth mentioning that SBS threshold for LP01 mode is lower than LP11 mode therefore, SBS suppression is not necessary in the pump 2 path. This arrangement would facilitate precise adjustment of the relative polarization between one pump and the seed and reduce SBS back reflection by broadening the spectrum of the beams. Following amplification through an erbium-doped fiber amplifier (EDFA) with an output power just below 27 dBm, a programmable optical filter is applied to enhance the signal-to-noise ratio and reduce the effect of the amplified spontaneous emission outside of the pump and seed wavelength. A second CW pump was also similarly set up to couple to a different modal input of the photonic lantern. The relative polarization between pump 2 and pump1 and seed could also be controlled with a polarization controller added to the pump 2 path.

IV. EXPERIMENTAL RESULTS

To see the various FWM effects of the fiber, we set the pumps' wavelengths at 1550 nm and 1551 nm, in LP₀₁ and LP₁₁ modes, respectively. Based on the phase matching

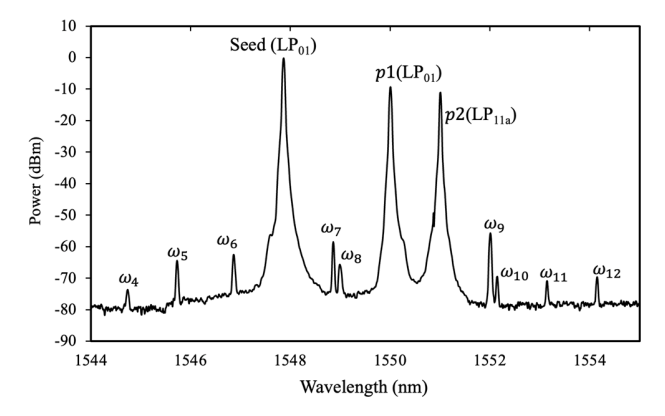


Fig. 2. Combined LP₁₁ output spectra of the FMF under test.

FWM Effects of Fig. 2 With $\lambda_1^{01}=1550nm$, $\lambda_2^{11}=1551$ nm, and $\lambda_3^{01}=1547.81$ nm

Effect	$\lambda (nm)$	P(dBm)	Process	$\Delta \beta (1/km)$
ω_4	1544.74	-73.65	$2\omega_3-\omega_2$	$\beta_4^{01} - \beta_3^{11} - \beta_3^{01} + \beta_2^{11} = 18.18$
ω_5	1545.73	-64.42	$2\omega_3-\omega_1$	$\beta_5^{01} - \beta_3^{11} - \beta_3^{01} + \beta_1^{11} = 44.17$
ω_6	1546.87	-62.6	$\omega_1 - \omega_2 + \omega_3$	$\beta_6^{01} - \beta_1^{11} + \beta_2^{11} - \beta_3^{01} = 5.75$
ω_7	1548.86	-58.5	$-\omega_1 + \omega_2 + \omega_3$	$\beta_7^{01} + \beta_3^{11} - \beta_3^{11} - \beta_1^{01} = -20.77$
ω8	1548.99	-65.68	$2\omega_1-\omega_2$	$\beta_8^{11} - 2\beta_1^{11} + \beta_2^{11} = -15$ $\beta_8^{01} - 2\beta_1^{01} + \beta_2^{01} = -15.46$
ω9	1552.01	-55.69	$2\omega_2-\omega_1$	$\beta_9^{11} - 2\beta_2^{11} + \beta_1^{11} = -15.09$ $\beta_9^{01} - 2\beta_2^{01} + \beta_1^{01} = -15.61$
ω_{10}	1552.15	-69.51	$2\omega_1-\omega_3$	$\beta_{10}^{11} - \beta_{1}^{11} - \beta_{1}^{01} + \beta_{3}^{01} = 44.27$
ω_{11}	1553.14	-70.96	$\omega_1 + \omega_2 - \omega_3$	$\beta_{11}^{11} - \beta_{1}^{01} - \beta_{2}^{11} + \beta_{3}^{01} = 13$
ω_{12}	1554.15	-69.63	$2\omega_2-\omega_3$	$\beta_{12}^{11} - \beta_2^{01} - \beta_2^{11} + \beta_3^{01} = 18.73$

equation in (1) for the SFWM process, the Stokes and anti-Stokes are expected at 1553.19 nm (in LP₁₁) and 1547.81 nm (in LP₀₁), respectively. This process is of great interest as it generates entangled photon pairs in the FMF within the C-band. Since the efficiency of the intermodal SFWM is low, the spontaneous effects are buried under the gain of the EDFAs. Therefore, we seeded the anti-Stokes beam at 1547.81 nm with a tunable CW laser in its corresponding mode (LP₀₁) and observed the LP₁₁ output of the mode demultiplexer as the Stokes photons should have an LP₁₁ spatial profile. Powers of 14.91 dBm, 5 dBm, and 14 dBm were launched into different channels of the multiplexer. The exact coupled power in each mode can be calculated after taking into account the insertion losses of the multiplexer channels. We used a 2×1 coupler to combine the LP_{11a} and LP_{11b} outputs of the demultiplexer as the fiber has degenerate LP₁₁ mode components. The spectral content of the combined demultiplexer channels is then acquired using an optical spectrum analyzer (OSA).

Fig. 2 demonstrates the results taken from the OSA at a 0.05 nm spectral resolution. Various FWM effects ($\omega_4 - \omega_{12}$) are observed in this output spectra, as shown in Fig. 2 and listed in Table I. ω_1, ω_2 , and ω_3 correspond to pump 1, pump 2, and seed frequencies. While the cross-mode coupling was reduced using active splicing, modal crosstalk still exists and results in strong fields in each mode evidenced by the spectral measurements. Therefore, we calculated (2) for various configurations and mode combinations of the involved spectral Authorized licensed use limited to: Missouri University of Science and Technology. Downloaded on May 13,2024 at 17:41:05 UTC from IEEE Xplore. Restrictions apply

TABLE II FWM Effects Observed in Fig. 3 With $\lambda_1^{01} = 1550 \, nm$, $\lambda_2^{11} = 1551 \text{ nm}, \text{ AND } \lambda_3^{11} = 1553.19 \text{ nm}$

Effect	$\lambda (nm)$	P(dBm)	Process	Δβ (1/km)
ω_4	1546.77	-71.73	$2\omega_1-\omega_3$	$\beta_4^{01} - \beta_1^{11} - \beta_1^{01} + \beta_3^{11} = 14.60$
ω_5	1547.77	-69.3	$\omega_1 + \omega_2 - \omega_3$	$\beta_5^{01} - \beta_1^{01} - \beta_2^{11} + \beta_3^{11} = 10.44$
ω_6	1548.78	-68	$2\omega_2-\omega_3$	$\beta_6^{01} - \beta_2^{01} + \beta_2^{11} - \beta_3^{11} = 44.09$
ω_7	1549	-64.06	$2\omega_1-\omega_2$	$\beta_7^{01} - 2\beta_1^{01} + \beta_2^{01} = -15.14$ $\beta_7^{11} - 2\beta_1^{11} + \beta_2^{11} = -15.15$
ω ₈	1552.01	-65.1	$2\omega_2-\omega_1$	$\beta_8^{11} - 2\beta_2^{11} + \beta_1^{11} = -14.49$ $\beta_8^{01} - 2\beta_2^{01} + \beta_1^{01} = -13.42$
ω_9	1552.24	-59.95	$\omega_1 - \omega_2 + \omega_3$	$\beta_9^{11} - \beta_1^{01} + \beta_2^{01} - \beta_3^{11} = -19.89$
ω_{10}	1554.26	-65.8	$-\omega_1 + \omega_2 + \omega_3$	$\beta_{10}^{11} + \beta_{1}^{01} - \beta_{1}^{01} - \beta_{3}^{11} = 4.93$
ω_{11}	1555.49	-65.8	$2\omega_3-\omega_2$	$\beta_{11}^{11} - \beta_{3}^{11} - \beta_{3}^{01} + \beta_{2}^{01} = 43.52$
ω_{12}	1556.5	-72.51	$2\omega_3-\omega_1$	$\beta_{12}^{11} - \beta_{3}^{11} - \beta_{3}^{01} + \beta_{1}^{01} = 15.48$

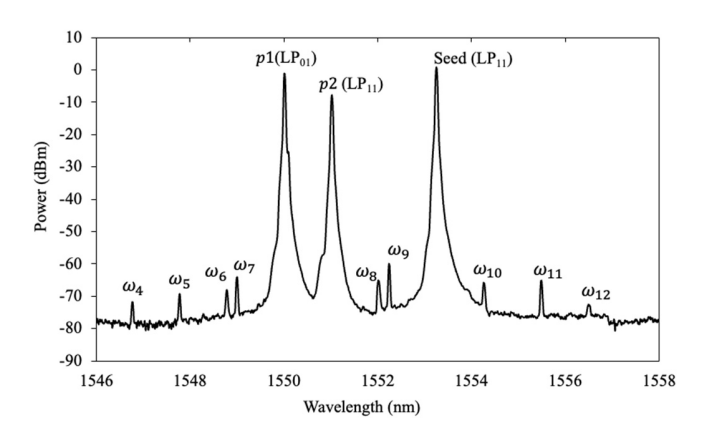


Fig. 3. LP₀₁ output spectra of the FMF under test.

components. The effects with the lowest phase mismatch are most likely to happen due to higher efficiency based on $sinc^2(\Delta\beta L/2)$ [5]. Among the processes listed in Table I, the process ω_{11} is the process that is predicted by (1). The phase mismatch, $\Delta \beta$, of this process is predicted to be zero, while the calculated phase mismatch value based on the experiment is equal to 13km⁻¹. This discrepancy might be due to a slight difference in the seed wavelength (measured to be 1547.86 nm while the theoretically calculated value is 1547.81 nm) accumulated over the 25 km length of the fiber. The effects designated as ω_4 , ω_5 , ω_{10} , and ω_{12} are intermodal processes. Their minimum phase mismatch values as well as the corresponding mode combination are provided in Table I. ω_8 and ω_9 are most likely to be intramodal effects having minimum $\Delta \beta$ values (maximum efficiencies) when all the waves are in LP_{01} or LP_{11} modes.

In a subsequent measurement, we seeded the Stokes process into LP₁₁ mode with a CW beam centered at 1553.19 nm and monitored the LP₀₁ output channel of the output demultiplexer. The spectral density of the LP_{01} output is shown in Fig. 3, and the peak profiles are summarized in Table II. Similarly, we have observed strong mode coupling between the FMF modes; therefore, multiple intermodal and intramodal processes are expected. Similar to the previous measurement of Fig. 2, in Fig. 3, we have observed nine FWM processes, and based on the phase mismatch of (2), processes ω_4, ω_6 , and $\omega_9 - \omega_{12}$ are all expected to be intermodal processes,

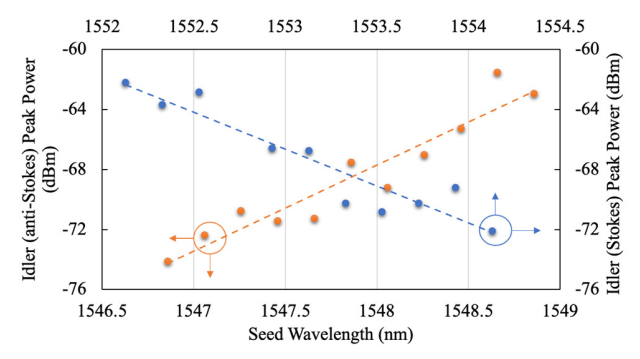


Fig. 4. Peak power of anti-Stokes and Stokes processes for various seed wavelengths at a constant total input power.

while processes of ω_7 and ω_8 are most likely intramodal processes between the two pumps. The phase mismatch of each process is calculated the mode combination that resulted in the minimum $\Delta\beta$ values are listed on Table II. The process corresponding to ω_5 is also the FWM process corresponding to (1). Similar to ω_{11} of Fig. 2, ω_5 of Fig. 3 with $\Delta\beta=10.44 {\rm km}^{-1}$ is an intermodal effect due to maximized efficiency at the intermodal configuration thanks to the minimized phase mismatch at the mode configuration for which the $\Delta\beta$ is calculated and listed in Table II.

Next, for the arrangement of Fig. 2, we swept the seed laser between 1546.5 - 1548.5 nm while keeping the two pumps at 1550 nm and 1551 nm. We monitored the peak power of the process designated as ω_{11} and plotted the results in Fig. 4(a). As observed from the graph, the efficiency of the seeded SFWM process increases by moving the seed closer to the two pumps, even though the phase mismatch is increasing. It has been demonstrated that, both theoretically and experimentally, intermodal FWM processes have a full width at half max of 3-5 nm [5], [6]. However, for this fiber, due to the limited dispersion group delay and a $\Delta \lambda = 3.2$ nm, the power increases as we move the seed away from the ideal phase-matched condition and closer to the pumps. We repeated this measurement for the ω_5 process of Fig. 3, where we observed the power of the ω_5 idler as we swept the seed wavelength between 1552-1554.5 nm. As shown in Fig. 4(b), a similar power increase is observed as the seed gets closer to the non-degenerate pumps.

V. CONCLUSION

We experimentally investigated the non-degenerate pump configuration for intermodal SFWM through the seeding technique due to the effect's extremely low efficiency. We seeded the Stokes or anti-Stokes frequencies for the ideal SFWM process and observed multiple stimulated FWM processes. We then identified each process through phase mismatch calculations; intermodal versus intramodal effects were distinguished based on their respective efficiencies. While we expected the intermodal effects to be maximized at the perfect phase-matched condition, we observed increasing efficiency as the seed got closer to the non-degenerate pumps. We attribute this to the low dispersion group delay between the fiber modes. Therefore, a fiber with a larger $\Delta\lambda$ is desirable to effectively filter out the pumps for optimized photon pair generation through intermodal SFWM.

ACKNOWLEDGMENT

The authors thank Dr. Rene-Jean Essiambre from Nokia Bell Laboratories for fruitful discussions.

REFERENCES

- [1] R. H. Stolen, J. E. Bjorkholm, and A. Ashkin, "Phase-matched three-wave mixing in silica fiber optical waveguides," *Appl. Phys. Lett.*, vol. 24, no. 7, pp. 308–310, Apr. 1974.
- [2] R.-J. Essiambre et al., "Experimental investigation of inter-modal four-wave mixing in few-mode fibers," *IEEE Photon. Technol. Lett.*, vol. 25, no. 6, pp. 539–542, Mar. 15, 2013.
- [3] J. Yuan et al., "Enhanced intermodal four-wave mixing for visible and near-infrared wavelength generation in a photonic crystal fiber," Opt. Lett., vol. 40, no. 7, p. 1338, Apr. 2015, doi: 10.1364/ol.40.001338.
- [4] S. R. Petersen, T. T. Alkeskjold, C. B. Olausson, and J. Lægsgaard, "Intermodal and cross-polarization four-wave mixing in large-core hybrid photonic crystal fibers," *Opt. Exp.*, vol. 23, no. 5, pp. 5954–5971, 2015. doi: 10.1364/OE.23.005954.
- [5] Y. Xiao et al., "Theory of intermodal four-wave mixing with random linear mode coupling in few-mode fibers," *Opt. Exp.*, vol. 22, no. 26, p. 32039, Dec. 2014, doi: 10.1364/oe.22.032039.
- [6] M. Esmaeelpour et al., "Power fluctuations of intermodal four-wave mixing in few-mode fibers," J. Lightw. Technol., vol. 35, no. 12, pp. 2429–2435, Jun. 15, 2017.
- [7] G. Rademacher et al., "Investigation of intermodal four-wave mixing for nonlinear signal processing in few-mode fibers," *IEEE Photon. Technol. Lett.*, vol. 30, no. 17, pp. 1527–1530, Sep. 1, 2018.
- [8] E. Nazemosadat, H. Pourbeyram, and A. Mafi, "Phase matching for spontaneous frequency conversion via four-wave mixing in graded-index multimode optical fibers," *J. Opt. Soc. Amer. B, Opt. Phys.*, vol. 33, no. 2, p. 144, Feb. 2016.
- [9] R. Dupiol et al., "Far-detuned cascaded intermodal four-wave mixing in a multimode fiber," *Opt. Lett.*, vol. 42, no. 7, p. 1293, Apr. 2017, doi: 10.1364/ol.42.001293.
- [10] F. Parmigiani et al., "All-optical mode and wavelength converter based on parametric processes in a three-mode fiber," *Opt. Exp.*, vol. 25, no. 26, p. 33602, Dec. 2017, doi: 10.1364/oe.25.033602.
- [11] C. Zhang, Y. Huang, B. Liu, C. Li, and G. Guo, "Spontaneous parametric down-conversion sources for multiphoton experiments," *Adv. Quantum Technol.*, vol. 4, no. 5, May 2021, Art. no. 2000132.
- [12] H. Takesue and K. Inoue, "Generation of polarization-entangled photon pairs and violation of Bell's inequality using spontaneous four-wave mixing in a fiber loop," *Phys. Rev. A, Gen. Phys.*, vol. 70, no. 3, Sep. 2004, Art. no. 031802, doi: 10.1103/physreva.70. 031802.
- [13] K. Rottwitt, J. Koefoed, and E. Christensen, "Photon-pair sources based on intermodal four-wave mixing in few-mode fibers," *Fibers*, vol. 6, no. 2, p. 32, May 2018, doi: 10.3390/fib6020032.
- [14] Ç. Ekici and M. S. Dinleyici, "Graded-index optical fiber transverse-spatial-mode entanglement," *Phys. Rev. A, Gen. Phys.*, vol. 102, no. 1, Jul. 2020, Art. no. 013702.
- [15] S. Majchrowska, K. Żołnacz, W. Urbańczyk, and K. Tarnowski, "Multiple intermodal-vectorial four-wave mixing bands generated by selective excitation of orthogonally polarized LP01 and LP11 modes in a birefringent fiber," Opt. Lett., vol. 47, no. 10, p. 2522, May 2022
- [16] K. Lee, J. Jung, and J. H. Lee, "Optical fiber polarization-entangled photon pair source using intermodal spontaneous four-wave mixing in the visible spectral band," *Laser Phys. Lett.*, vol. 20, no. 1, Dec. 2022, Art. no. 015101.
- [17] C. Guo, J. Su, Z. Zhang, L. Cui, and X. Li, "Generation of telecomband correlated photon pairs in different spatial modes using few-mode fibers," Opt. Lett., vol. 44, no. 2, p. 235, Jan. 2019.
- [18] A. Shamsshooli, C. Guo, F. Parmigiani, X. Li, and M. Vasilyev, "Progress toward spatially-entangled photon-pair generation in a few-mode fiber," *IEEE Photon. Technol. Lett.*, vol. 33, no. 16, pp. 864–867, Aug. 15, 2021.
- [19] S. Montazeri and M. Esmaeelpour, "Entangled photon pair generation via spontaneous intermodal four-wave mixing in a 25-km-long few-mode fiber," *Proc. SPIE*, vol. 12446, Mar. 2023, Art. no. 124460W.
- [20] R.-J. Essiambre et al., "Experimental observation of inter-modal crossphase modulation in few-mode fibers," *IEEE Photon. Technol. Lett.*, vol. 25, no. 6, pp. 535–538, Mar. 15, 2013.